Appl Phys B (2010) 101: 371–379
DOI 10.1007/s00340-010-3974-1

Applied Physics B
Lasers and Optics

Average intensity and spreading of super Lorentz–Gauss modes in turbulent atmosphere

G. Zhou

Received: 5 January 2010 / Revised version: 16 February 2010 / Published online: 16 March 2010

Abstract The super Lorentz–Gaussian (SLG) modes has been introduced to describe the radiation emitted by the multi-mode diode lasers. Here the propagation properties of SLG modes in turbulent atmosphere are investigated. Based on the extended Huygens–Fresnel integral and the Hermite–Gaussian expansion of a Lorentzian function, analytical formulae for the average intensities and the effective beam sizes of SLG_{01} and SLG_{11} modes are derived in turbulent atmosphere. The average intensity distribution and the spreading properties of SLG_{01} and SLG_{11} modes in turbulent atmosphere are numerically demonstrated. The influences of the beam parameters and the structure constant of the atmospheric turbulence on the propagation of SLG_{01} and SLG_{11} modes in turbulent atmosphere are also discussed in detail.

1 Introduction

As the angular spreading of a Lorentz–Gaussian distribution is higher than that of a Gaussian distribution, Lorentz–Gaussian beams provide more appropriate models than Gaussian beams to describe the radiation emitted by a single mode diode laser [1, 2]. In the limiting case, Lorentz–Gaussian beams reduce to Lorentz beams. Within the framework of the paraxial and non-paraxial cases, the properties of Lorentz–Gaussian beams have been extensively investigated [3–11]. The researches show that Lorentz–Gaussian beams are only applicable to the description of the fundamental mode emitted by a single mode diode laser. However, the high power diode lasers also generate the higher-order modes. How can we describe the radiation emitted by the multi-mode diode lasers? An orthonormal family of super Lorentz–Gaussian (SLG) modes has been introduced to describe the radiation emitted by the multi-mode diode lasers [12]. Due to applications in free-space optical communications and remote sensing, the propagation of various kinds of laser beams in a turbulent atmosphere has been extensively investigated [13–22]. To the best of our knowledge, the propagation of SLG modes in turbulent atmosphere has not been reported. Here, we mainly pay attention to the simple case, where only SLG_{01} and SLG_{11} modes are considered. In the remainder of this paper, therefore, the propagation of SLG_{01} and SLG_{11} modes is examined in turbulent atmosphere. Analytical propagation formulae of the average intensities and the effective beam sizes of SLG_{01} and SLG_{11} modes in turbulent atmosphere are derived by means of the mathematical techniques. Also, the numerical calculations are carried out to illustrate the influences of the beam parameters and the structure constant on the propagation of SLG_{01} and SLG_{11} modes in turbulent atmosphere.

2 Propagation of SLG_{01} and SLG_{11} modes in turbulent atmosphere

In the Cartesian coordinate system, the z-axis is taken to be the propagation axis. The SLG modes in the source plane $z = 0$ take the form [12]:

$$E(\boldsymbol{r}_0, 0) = E_m(x_0, 0) E_{m'}(y_0, 0), \tag{1}$$

with $E_m(x_0, 0)$ and $E_{m'}(y_0, 0)$ given by

$$E_{2p}(j_0, 0) = \exp\left(-\frac{j_0^2}{w_0^2}\right)\left(j_0^{2p} + \sum_{q=1}^{p-1} c_{(2p)(2q)} j_0^{2l}\right)$$

G. Zhou (✉)
School of Sciences, Zhejiang Forestry University, Lin'an 311300, Zhejiang Province, China
e-mail: zhouguoquan178@sohu.com

$$\times \prod_{s=1}^{M} \frac{1}{j_0^2 + \alpha_{(s-1)j}^2}, \tag{2}$$

$$E_{2p+1}(j_0, 0) = \exp\left(-\frac{j_0^2}{w_0^2}\right)\left(j_0^{2p+1} + \sum_{q=1}^{p-1} c_{(2p+1)(2q+1)} j_0^{2l+1}\right) \times \prod_{s=1}^{M} \frac{1}{j_0^2 + \alpha_{(s-1)j}^2}, \tag{3}$$

where $\boldsymbol{r}_0 = x_0\mathbf{e}_x + y_0\mathbf{e}_y$. $\mathbf{e}_x$ and $\mathbf{e}_y$ are the two transverse unit vectors in the Cartesian coordinate system, respectively. $j = x$ or y (hereafter). m and m' are arbitrary integers. w_0 is the waist of the Gaussian part. M is an integer, and $p = 0, \dots, M-1$. $c_{(2p)(2q)}$ and $c_{(2p+1)(2q+1)}$ are coefficients calculated by the method suggested by [4]. $\alpha_{(s-1)j}$ is the parameter related to the beam width of the super-Lorentzian part in the j-direction. In case of $M = 1$, there are four mutually orthogonal SLG modes, namely SLG_{00}, SLG_{01}, SLG_{10}, and SLG_{11} modes:

$$E^{00}(\boldsymbol{r}_0, 0) = \frac{2}{\pi\alpha_{0x}^{1/2}\alpha_{0y}^{1/2}} \frac{1}{[1 + (x_0/\alpha_{0x})^2][1 + (y_0/\alpha_{0y})^2]} \times \exp\left(-\frac{x_0^2 + y_0^2}{w_0^2}\right), \tag{4}$$

$$E^{01}(\boldsymbol{r}_0, 0) = \frac{2}{\pi\alpha_{0x}^{1/2}\alpha_{0y}^{3/2}} \frac{y_0}{[1 + (x_0/\alpha_{0x})^2][1 + (y_0/\alpha_{0y})^2]} \times \exp\left(-\frac{x_0^2 + y_0^2}{w_0^2}\right), \tag{5}$$

$$E^{10}(r_0, 0) = \frac{2}{\pi\alpha_{0x}^{3/2}\alpha_{0y}^{1/2}} \frac{x_0}{[1 + (x_0/\alpha_{0x})^2][1 + (y_0/\alpha_{0y})^2]} \times \exp\left(-\frac{x_0^2 + y_0^2}{w_0^2}\right), \tag{6}$$

$$E^{11}(r_0, 0) = \frac{2}{\pi\alpha_{0x}^{3/2}\alpha_{0y}^{3/2}} \frac{x_0 y_0}{[1 + (x_0/\alpha_{0x})^2][1 + (y_0/\alpha_{0y})^2]} \times \exp\left(-\frac{x_0^2 + y_0^2}{w_0^2}\right). \tag{7}$$

The mentioned SLG beams possess the same rectangular symmetry as Hermite–Gaussian beams with the same indices. The SLG_{00} mode is just the Lorentz–Gaussian beam and has been extensively investigated. As to the SLG_{10} mode, it can be obtained by exchange of x and y in the field expression of SLG_{01} mode. Therefore, here we only consider SLG_{01} and SLG_{11} modes. The time-dependent factor $\exp(-i\omega t)$ is omitted in the (1) where ω is the circular frequency. The Lorentz distribution can be expanded into the linear superposition of Hermite–Gaussian functions [23]:

$$\frac{y_0}{(x_0^2 + \alpha_{0x}^2)(y_0^2 + \alpha_{0y}^2)} = \frac{\pi}{4\alpha_{0x}^2\alpha_{0y}} \sum_{n=0}^{N}\sum_{n'=0}^{N} a_{2n}a_{2n'} H_{2n}\left(\frac{x_0}{\alpha_{0x}}\right) \times \left[H_{2n'+1}\left(\frac{y_0}{\alpha_{0y}}\right) + 4n' H_{2n'-1}\left(\frac{y_0}{\alpha_{0y}}\right)\right] \times \exp\left(-\frac{x_0^2}{\alpha_{0x}^2} - \frac{y_0^2}{\alpha_{0y}^2}\right), \tag{8}$$

$$\frac{x_0 y_0}{(x_0^2 + \alpha_{0x}^2)(y_0^2 + \alpha_{0y}^2)} = \frac{\pi}{8\alpha_{0x}\alpha_{0y}} \sum_{n=0}^{N}\sum_{n'=0}^{N} a_{2n}a_{2n'} \times \left[H_{2n+1}\left(\frac{x_0}{\alpha_{0x}}\right) + 4n H_{2n-1}\left(\frac{x_0}{\alpha_{0x}}\right)\right] \times \left[H_{2n'+1}\left(\frac{y_0}{\alpha_{0y}}\right) + 4n' H_{2n'-1}\left(\frac{y_0}{\alpha_{0y}}\right)\right] \times \exp\left(-\frac{x_0^2}{\alpha_{0x}^2} - \frac{y_0^2}{\alpha_{0y}^2}\right), \tag{9}$$

where N is the number of the expansion. a_{2n} and $a_{2n'}$ are the weight coefficients and can be indexed in [23]. $H_{2n}(.)$ is the $2n$th-order Hermite polynomial. In the derivation of above equations, the following mathematical formula is used [24]:

$$2xH_n(x) = H_{n+1}(x) + 2nH_{n-1}(x). \tag{10}$$

Therefore, (5) and (7) can be rewritten as follows:

$$E^{01}(\boldsymbol{r}_0, 0) = \frac{1}{2\alpha_{0x}^{1/2}\alpha_{0y}^{1/2}} \sum_{n=0}^{N}\sum_{n'=0}^{N} a_{2n}a_{2n'} H_{2n}\left(\frac{x_0}{\alpha_{0x}}\right) \times \left[H_{2n'+1}\left(\frac{y_0}{\alpha_{0y}}\right) + 4n' H_{2n'-1}\left(\frac{y_0}{\alpha_{0y}}\right)\right] \times \exp\left(-\frac{x_0^2}{w_x^2} - \frac{y_0^2}{w_y^2}\right), \tag{11}$$

$$E^{11}(\boldsymbol{r}_0, 0) = \frac{1}{4\alpha_{0x}^{1/2}\alpha_{0y}^{1/2}} \sum_{n=0}^{N}\sum_{n'=0}^{N} a_{2n}a_{2n'} \times \left[H_{2n+1}\left(\frac{x_0}{\alpha_{0x}}\right) + 4n H_{2n-1}\left(\frac{x_0}{\alpha_{0x}}\right)\right] \times \left[H_{2n'+1}\left(\frac{y_0}{\alpha_{0y}}\right) + 4n' H_{2n'-1}\left(\frac{y_0}{\alpha_{0y}}\right)\right]$$

$$\times \exp\left(-\frac{x_0^2}{w_x^2}-\frac{y_0^2}{w_y^2}\right), \tag{12}$$

where

$$\frac{1}{w_j^2}=\frac{1}{w_0^2}+\frac{1}{2\alpha_{0j}^2}. \tag{13}$$

The propagation of SLG_{01} and SLG_{11} modes in a turbulent atmosphere can be investigated by using the following extended Huygens–Fresnel integral:

$$E(\boldsymbol{r},z)=-\frac{ik}{2\pi z}\int_{-\infty}^{\infty}\int_{-\infty}^{\infty}E(\boldsymbol{r}_0,0) \times \exp\left[-\frac{ik}{2z}(\boldsymbol{r}_0-\boldsymbol{r})^2+\psi(\boldsymbol{r}_0,\boldsymbol{r})\right]dx_0\,dy_0, \tag{14}$$

where $\boldsymbol{r}=x\mathbf{e}_x+y\mathbf{e}_y$. $(\boldsymbol{r},z)$ is the receiver plane. $\psi(\boldsymbol{r}_0,\boldsymbol{r})$ is the solution to the Rytov method that represents the random part of the complex phase. $k=2\pi/\lambda$ is the wave number. λ is the optical wavelength. The average intensities of SLG_{01} and SLG_{11} modes in the receiver plane are given by

$$\langle I(\boldsymbol{r},z)\rangle=\frac{k^2}{4\pi^2z^2}\int_{-\infty}^{\infty}\int_{-\infty}^{\infty}\int_{-\infty}^{\infty}\int_{-\infty}^{\infty}E(\boldsymbol{r}_{01},0)E^*(\boldsymbol{r}_{02},0) \times \exp\left[-\frac{ik}{2z}(\boldsymbol{r}_{01}-\boldsymbol{r})^2+\frac{ik}{2z}(\boldsymbol{r}_{02}-\boldsymbol{r})^2\right] \times \langle\exp[\psi(\boldsymbol{r}_{01},\boldsymbol{r})+\psi^*(\boldsymbol{r}_{02},\boldsymbol{r})]\rangle d\boldsymbol{r}_{01}\,d\boldsymbol{r}_{02}, \tag{15}$$

where the angle brackets indicate the ensemble average over the medium statistics, and the asterisk denotes the complex conjugation. The last ensemble average term in the above equation can be expressed as follow:

$$\langle\exp[\psi(\boldsymbol{r}_{01},\boldsymbol{r})+\psi^*(\boldsymbol{r}_{02},\boldsymbol{r})]\rangle =\exp[-0.5D_\psi(\boldsymbol{r}_{01}-\boldsymbol{r}_{02})]=\exp\left[-\frac{(\boldsymbol{r}_{01}-\boldsymbol{r}_{02})^2}{\rho_0^2}\right], \tag{16}$$

where $D_\psi(\boldsymbol{r}_{01}-\boldsymbol{r}_{02})$ is the phase function in Rytov's representation and $\rho_0=(0.545C_n^2k^2z)^{-3/5}$ is the spherical wave lateral coherence length. C_n^2 is the structure constant of the atmospheric turbulence. Substituting (11) and (12) into (15) and using the following mathematical formulae [24]:

$$\int_{-\infty}^{\infty}H_{n'}(x)\exp\left[-\frac{(x-y)^2}{u}\right]dx =\sqrt{\frac{\pi}{u}}(1-u)^{n'/2}H_{n'}\left(\frac{y}{\sqrt{1-u}}\right), \tag{17}$$

$$H_n(x)=\sum_{l=0}^{[\frac{n}{2}]}\frac{(-1)^l(n)!}{l!(n-2l)!}(2x)^{n-2l}, \tag{18}$$

$$\int_{-\infty}^{\infty}x^n\exp(-bx^2+2cx)\,dx =n!\sqrt{\frac{\pi}{b}}\left(\frac{c}{b}\right)^n\exp\left(\frac{c^2}{b}\right)\sum_{s=0}^{[\frac{n}{2}]}\frac{1}{s!(n-2s)!}\left(\frac{b}{4c^2}\right)^s, \tag{19}$$

where $[n/2]$ gives the greatest integer less than or equal to $n/2$, we can obtain the analytical average intensities of SLG_{01} and SLG_{11} modes in the receiver plane:

$$\langle I^{01}(\boldsymbol{r},z)\rangle=\langle I^0(x,z)\rangle\langle I^1(y,z)\rangle, \tag{20}$$

$$\langle I^{11}(\boldsymbol{r},z)\rangle=\langle I^1(x,z)\rangle\langle I^1(y,z)\rangle, \tag{21}$$

with $\langle I^0(x,z)\rangle$ and $\langle I^1(j,z)\rangle$ given by

$$\langle I^0(x,z)\rangle =\frac{k\alpha_{0x}}{2z}\sqrt{\frac{1}{b_{1x}b_{2x}}}\exp\left(\frac{c_x^2}{b_{2x}}-\frac{k^2\alpha_{0x}^2x^2}{4b_{1x}z^2}\right) \times\sum_{n=0}^{N}\sum_{n'=0}^{N}a_{2n}a_{2n'}\left(1-\frac{1}{b_{1x}}\right)^{n'}\sum_{l_1=0}^{n}\frac{(-1)^{l_1}(2n)!}{l_1!(2n-2l_1)!} \times\sum_{l_2=0}^{n'}\frac{(-1)^{l_2}(2n')!}{l_2!(2n'-2l_2)!}\sum_{l_3=0}^{2n'-2l_2}\binom{2n'-2l_2}{l_3} \times 2^{2(n+n')-2l_1-2l_2}e_x^{l_3}h_x^{2n'-2l_2-l_3}(2n+l_3-2l_1)! \times\left(\frac{c_x}{b_{2x}}\right)^{2n+l_3-2l_1}\sum_{s=0}^{[\frac{2n+l_3-2l_1}{2}]}\frac{1}{s!(2n+l_3-2l_1-2s)!} \times\left(\frac{b_{2x}}{4c_x^2}\right)^s, \tag{22}$$

$$\langle I^1(j,z)\rangle=\beta_1(j,z)+\beta_2(j,z)+\beta_3(j,z)+\beta_4(j,z), \tag{23}$$

$$\beta_1(j,z) =\frac{k\alpha_{0j}}{8z}\sqrt{\frac{1}{b_{1j}b_{2j}}}\exp\left(\frac{c_j^2}{b_{2j}}-\frac{k^2\alpha_{0j}^2j^2}{4b_{1j}z^2}\right) \times\sum_{n=0}^{N}\sum_{n'=0}^{N}a_{2n}a_{2n'}\left(1-\frac{1}{b_{1j}}\right)^{(2n'+1)/2} \times\sum_{l_1=0}^{[\frac{2n+1}{2}]}\frac{(-1)^{l_1}(2n+1)!}{l_1!(2n+1-2l_1)!} \times\sum_{l_2=0}^{[\frac{2n'+1}{2}]}\frac{(-1)^{l_2}(2n'+1)!}{l_2!(2n'+1-2l_2)!}$$

$$\times \sum_{l_3=0}^{2n'+1-2l_2} \binom{2n'+1-2l_2}{l_3} \times 2^{2(n+n'+1)-2l_1-2l_2} e_j^{l_3} h_j^{2n'+1-2l_2-l_3} \times (2n+l_3+1-2l_1)! \left(\frac{c_j}{b_{2j}}\right)^{2n+l_3+1-2l_1} \times \sum_{s=0}^{[\frac{2n+l_3+1-2l_1}{2}]} \frac{1}{s!(2n+l_3+1-2l_1-2s)!} \left(\frac{b_{2j}}{4c_j^2}\right)^s, \tag{24}$$

$$\beta_2(j,z) = \frac{k\alpha_{0j}}{2z}\sqrt{\frac{1}{b_{1j}b_{2j}}} \exp\left(\frac{c_j^2}{b_{2j}} - \frac{k^2\alpha_{0j}^2 j^2}{4b_{1j}z^2}\right) \times \sum_{n=0}^{N}\sum_{n'=1}^{N} n' a_{2n} a_{2n'} \left(1-\frac{1}{b_{1j}}\right)^{(2n'-1)/2} \times \sum_{l_1=0}^{[\frac{2n+1}{2}]} \frac{(-1)^{l_1}(2n+1)!}{l_1!(2n+1-2l_1)!} \sum_{l_2=0}^{[\frac{2n'-1}{2}]} \frac{(-1)^{l_2}(2n'-1)!}{l_2!(2n'-2l_2-1)!} \times \sum_{l_3=0}^{2n'-2l_2-1} \binom{2n'-2l_2-1}{l_3} \times 2^{2(n+n')-2l_1-2l_2} e_j^{l_3} h_j^{2n'-2l_2-l_3-1} (2n+l_3+1-2l_1)! \times \left(\frac{c_j}{b_{2j}}\right)^{2n+l_3+1-2l_1} \sum_{s=0}^{[\frac{2n+l_3+1-2l_1}{2}]} \times \frac{1}{s!(2n+l_3+1-2l_1-2s)!} \left(\frac{b_{2j}}{4c_j^2}\right)^s, \tag{25}$$

$$\beta_3(j,z) = \frac{k\alpha_{0j}}{2z}\sqrt{\frac{1}{b_{1j}b_{2j}}} \exp\left(\frac{c_j^2}{b_{2j}} - \frac{k^2\alpha_{0j}^2 j^2}{4b_{1j}z^2}\right) \times \sum_{n=1}^{N}\sum_{n'=0}^{N} n a_{2n} a_{2n'} \left(1-\frac{1}{b_{1j}}\right)^{(2n'+1)/2} \times \sum_{l_1=0}^{[\frac{2n-1}{2}]} \frac{(-1)^{l_1}(2n-1)!}{l_1!(2n-2l_1-1)!} \sum_{l_2=0}^{[\frac{2n'+1}{2}]} \frac{(-1)^{l_2}(2n'+1)!}{l_2!(2n'+1-2l_2)!} \times \sum_{l_3=0}^{2n'+1-2l_2} \binom{2n'+1-2l_2}{l_3} \times 2^{2(n+n')-2l_1-2l_2} e_j^{l_3} h_j^{2n'+1-2l_2-l_3} (2n+l_3-2l_1-1)! \times \left(\frac{c_j}{b_{2j}}\right)^{2n+l_3-2l_1-1} \times \sum_{s=0}^{[\frac{2n+l_3-2l_1-1}{2}]} \frac{1}{s!(2n+l_3-2l_1-2s-1)!} \left(\frac{b_{2j}}{4c_j^2}\right)^s, \tag{26}$$

$$\beta_4(j,z) = \frac{2k\alpha_{0j}}{z}\sqrt{\frac{1}{b_{1j}b_{2j}}} \exp\left(\frac{c_j^2}{b_{2j}} - \frac{k^2\alpha_{0j}^2 j^2}{4b_{1j}z^2}\right) \times \sum_{n=1}^{N}\sum_{n'=1}^{N} nn' a_{2n} a_{2n'} \left(1-\frac{1}{b_{1j}}\right)^{(2n'-1)/2} \times \sum_{l_1=0}^{[\frac{2n-1}{2}]} \frac{(-1)^{l_1}(2n-1)!}{l_1!(2n-2l_1-1)!} \sum_{l_2=0}^{[\frac{2n'-1}{2}]} \frac{(-1)^{l_2}(2n'-1)!}{l_2!(2n'-2l_2-1)!} \times \sum_{l_3=0}^{2n'-2l_2-1} \binom{2n'-2l_2-1}{l_3} \times 2^{2(n+n'-1)-2l_1-2l_2} e_j^{l_3} h_j^{2n'-2l_2-l_3-1} \times (2n+l_3-2l_1-1)! \left(\frac{c_j}{b_{2j}}\right)^{2n+l_3-2l_1-1} \times \sum_{s=0}^{[\frac{2n+l_3-2l_1-1}{2}]} \frac{1}{s!(2n+l_3-2l_1-2s-1)!} \left(\frac{b_{2j}}{4c_j^2}\right)^s, \tag{27}$$

where

$$b_{1j} = \left(\frac{1}{w_j^2} + \frac{1}{\rho_0^2} - \frac{ik}{2z}\right)\alpha_{0j}^2,$$

$$b_{2j} = \left(\frac{1}{w_j^2} + \frac{1}{\rho_0^2} + \frac{ik}{2z}\right)\alpha_{0j}^2 - \frac{\alpha_{0j}^4}{b_{1j}\rho_0^4}, \tag{28}$$

$$c_j = \frac{ik\alpha_{0j} j}{2z} - \frac{ik\alpha_{0j}^3 j}{2zb_{1j}\rho_0^2},$$

$$e_j = \frac{\alpha_{0j}^2}{(b_{1j}^2 - b_{1j})^{1/2}\rho_0^2}, \qquad h_j = \frac{k\alpha_{0j} j}{2iz(b_{1j}^2 - b_{1j})^{1/2}}. \tag{29}$$

The effective beam sizes of SLG_{01} and SLG_{11} modes in the x- and y-directions of the receiver plane are defined as [21]

$$W_{jz} = \sqrt{\frac{2\int_{-\infty}^{\infty}\int_{-\infty}^{\infty} j^2 \langle I(\boldsymbol{r},z)\rangle\, dx\, dy}{\int_{-\infty}^{\infty}\int_{-\infty}^{\infty} \langle I(\boldsymbol{r},z)\rangle\, dx\, dy}}. \tag{30}$$

Substituting (20) and (21) into (30), the analytical effective beam sizes of SLG_{01} and SLG_{11} modes yield

$$W_{xz}^{0}=\sqrt{\frac{2A_x(1.5)}{A_x(0.5)}}, \quad (31)$$

$$W_{jz}^{1}=\sqrt{2\frac{B_{1j}(2.5)+B_{2j}(1.5)+B_{3j}(1.5)+B_{4j}(0.5)}{B_{1j}(1.5)+B_{2j}(0.5)+B_{3j}(0.5)+B_{4j}(-0.5)}}, \quad (32)$$

with $A_x(1.5)$, $A_x(0.5)$, $B_{1j}(2.5)$, $B_{2j}(1.5)$, $B_{3j}(1.5)$, $B_{4j}(0.5)$, $B_{1j}(1.5)$, $B_{2j}(0.5)$, $B_{3j}(0.5)$, and $B_{4j}(-0.5)$ given by

$$\begin{aligned}A_x(v_0)&=\sum_{n=0}^{N}\sum_{n'=0}^{N}a_{2n}a_{2n'}\left(1-\frac{1}{b_{1x}}\right)^{n'}\\&\times\sum_{l_1=0}^{n}\frac{(-1)^{l_1}(2n)!}{l_1!(2n-2l_1)!}\sum_{l_2=0}^{n'}\frac{(-1)^{l_2}(2n')!}{l_2!(2n'-2l_2)!}\\&\times\sum_{l_3=0}^{2n'-2l_2}\binom{2n'-2l_2}{l_3}2^{2(n+n')-2l_1-2l_2}\\&\times e_x^{l_3}\eta_x^{2n'-2l_2-l_3}(2n+l_3-2l_1)!\\&\times\sum_{s=0}^{[\frac{2n+l_3-2l_1}{2}]}\frac{1}{s!(2n+l_3-2l_1-2s)!4^s}\\&\times b_{2x}^{2l_1+s-2n-l_3}\xi_x^{2n+l_3-2l_1-2s}\\&\times\Gamma(n+n'-l_1-l_2-s+v_0)\zeta_x^{l_1+l_2+s-n-n'-v_0},\\&v_0=1.5\text{ or }0.5,\end{aligned} \quad (33)$$

$$\begin{aligned}B_{1j}(v_1)&=\sum_{n=0}^{N}\sum_{n'=0}^{N}a_{2n}a_{2n'}\left(1-\frac{1}{b_{1j}}\right)^{(2n'+1)/2}\\&\times\sum_{l_1=0}^{[\frac{2n+1}{2}]}\frac{(-1)^{l_1}(2n+1)!}{l_1!(2n+1-2l_1)!}\sum_{l_2=0}^{[\frac{2n'+1}{2}]}\frac{(-1)^{l_2}(2n'+1)!}{l_2!(2n'+1-2l_2)!}\\&\times\sum_{l_3=0}^{2n'+1-2l_2}\binom{2n'+1-2l_2}{l_3}2^{2(n+n'+1)-2l_1-2l_2}e_j^{l_3}\\&\times\eta_j^{2n'+1-2l_2-l_3}(2n+l_3+1-2l_1)!\\&\times\sum_{s=0}^{[\frac{2n+l_3+1-2l_1}{2}]}\frac{1}{s!(2n+l_3+1-2l_1-2s)!4^s}\\&\times b_{2j}^{2l_1+s-2n-l_3-1}\xi_j^{2n+l_3+1-2l_1-2s}\\&\times\Gamma(n+n'-l_1-l_2-s+v_1)\\&\times\zeta_j^{l_1+l_2+s-n-n'-v_1},\quad v_1=2.5\text{ or }1.5,\end{aligned} \quad (34)$$

$$\begin{aligned}B_{2j}(v_0)&=4\sum_{n=0}^{N}\sum_{n'=1}^{N}n'a_{2n}a_{2n'}\left(1-\frac{1}{b_{1j}}\right)^{(2n'-1)/2}\\&\times\sum_{l_1=0}^{[\frac{2n+1}{2}]}\frac{(-1)^{l_1}(2n+1)!}{l_1!(2n+1-2l_1)!}\sum_{l_2=0}^{[\frac{2n'-1}{2}]}\frac{(-1)^{l_2}(2n'-1)!}{l_2!(2n'-2l_2-1)!}\\&\times\sum_{l_3=0}^{2n'-2l_2-1}\binom{2n'-2l_2-1}{l_3}\\&\times 2^{2(n+n')-2l_1-2l_2}e_j^{l_3}\eta_j^{2n'-2l_2-l_3-1}\\&\times(2n+l_3+1-2l_1)!\\&\times\sum_{s=0}^{[\frac{2n+l_3+1-2l_1}{2}]}\frac{1}{s!(2n+l_3+1-2l_1-2s)!4^s}\\&\times b_{2j}^{2l_1+s-2n-l_3-1}\xi_j^{2n+l_3+1-2l_1-2s}\\&\times\Gamma(n+n'-l_1-l_2-s+v_0)\zeta_j^{l_1+l_2+s-n-n'-v_0},\end{aligned} \quad (35)$$

$$\begin{aligned}B_{3j}(v_0)&=4\sum_{n=1}^{N}\sum_{n'=0}^{N}na_{2n}a_{2n'}\left(1-\frac{1}{b_{1j}}\right)^{(2n'+1)/2}\\&\times\sum_{l_1=0}^{[\frac{2n-1}{2}]}\frac{(-1)^{l_1}(2n-1)!}{l_1!(2n-2l_1-1)!}\sum_{l_2=0}^{[\frac{2n'+1}{2}]}\frac{(-1)^{l_2}(2n'+1)!}{l_2!(2n'+1-2l_2)!}\\&\times\sum_{l_3=0}^{2n'+1-2l_2}\binom{2n'+1-2l_2}{l_3}\\&\times 2^{2(n+n')-2l_1-2l_2}e_j^{l_3}\eta_j^{2n'+1-2l_2-l_3}\\&\times(2n+l_3-2l_1-1)!\\&\times\sum_{s=0}^{[\frac{2n+l_3-2l_1-1}{2}]}\frac{1}{s!(2n+l_3-2l_1-2s-1)!4^s}\\&\times b_{2j}^{2l_1+s+1-2n-l_3}\xi_j^{2n+l_3-1-2l_1-2s}\\&\times\Gamma(n+n'-l_1-l_2-s+v_0)\zeta_j^{l_1+l_2+s-n-n'-v_0},\end{aligned} \quad (36)$$

$$B_{4j}(v_2)=16\sum_{n=1}^{N}\sum_{n'=1}^{N}nn'a_{2n}a_{2n'}\left(1-\frac{1}{b_{1j}}\right)^{(2n'-1)/2}$$

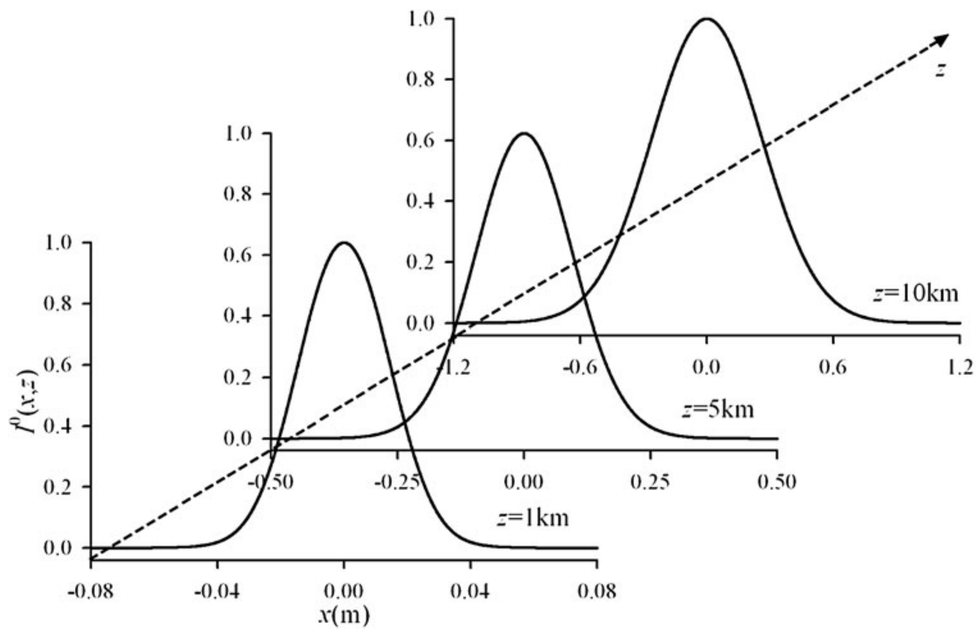

Fig. 1 Normalized average intensity distributions in the x-direction of a SLG_{01} mode at different propagation distances in turbulent atmosphere. $w_0 = 2$ cm, $\alpha_{0x} = 1$ cm, and $C_n^2 = 10^{-14}$ m$^{-2/3}$

$$\times \sum_{l_1=0}^{[\frac{2n-1}{2}]} \frac{(-1)^{l_1}(2n-1)!}{l_1!(2n-2l_1-1)!} \sum_{l_2=0}^{[\frac{2n'-1}{2}]} \frac{(-1)^{l_2}(2n'-1)!}{l_2!(2n'-2l_2-1)!}$$
$$\times \sum_{l_3=0}^{2n'-2l_2-1} \binom{2n'-2l_2-1}{l_3} 2^{2(n+n'-1)-2l_1-2l_2} e_j^{l_3}$$
$$\times \eta_j^{2n'-2l_2-l_3-1}(2n+l_3-2l_1-1)!$$
$$\times \sum_{s=0}^{[\frac{2n+l_3-2l_1-1}{2}]} \frac{1}{s!(2n+l_3-2l_1-2s-1)!4^s}$$
$$\times b_{2j}^{2l_1+s+1-2n-l_3} \xi_j^{2n+l_3-2l_1-2s-1}$$
$$\times \Gamma(n+n'-l_1-l_2-s+v_2)$$
$$\times \zeta_j^{l_1+l_2+s-n-n'-v_2}, \quad v_2 = 0.5 \text{ or } -0.5, \tag{37}$$

where

$$\eta_j = \frac{k\alpha_{0j}}{2iz(b_{1j}^2 - b_{1j})^{1/2}}, \qquad \xi_j = \frac{ik\alpha_{0j}}{2z} - \frac{ik\alpha_{0j}^3}{2zb_{1j}\rho_0^2},$$
$$\zeta_j = \frac{k^2\alpha_{0j}^2}{4b_{1j}z^2} - \frac{\xi_j^2}{b_{2j}}, \tag{38}$$

and $\Gamma(.)$ is a Gamma function.

3 Numerical calculations and analyses

Now, the average intensity and spreading of SLG_{01} and SLG_{11} modes in turbulent atmosphere are numerically calculated by using the formulae derived above. First, we consider the average intensity and spreading of a SLG_{01} mode in turbulent atmosphere. Figures 1 and 2 represent the normalized intensity distributions in the x- and y-directions of a SLG_{01} mode at several different propagation distances in turbulent atmosphere. The wavelength λ is set to be 0.8 μm (hereafter), and the structure constant C_n^2 is chosen as 10^{-14} m$^{-2/3}$. In Fig. 1, $w_0 = 2$ cm and $\alpha_{0x} = 1$ cm. In Fig. 2, $w_0 = 2$ cm and $\alpha_{0y} = 1$ cm. The beam profile in the x-direction of a SLG_{01} mode remains invariant upon propagation in turbulent atmosphere, though the corresponding beam spot in the x-direction expands upon propagation. However, the beam profile in the y-direction of a SLG_{01} mode essentially changes upon propagation in turbulent atmosphere. Due to the isotropic influence of the atmosphere turbulence, the vale in the normalized intensity distribution in the y-direction of a SLG_{01} mode gradually raises and finally disappears with increasing the propagation distance z. In the far field, the beam profile in the y-direction of a SLG_{01} mode tends to a Gaussian distribution. As the normalized intensity distribution of a SLG_{11} mode is same as that in the y-direction of a SLG_{01} mode, the corresponding figures are omitted to save space. For the sake of intuition, the contour graphs of normalized intensity distributions of SLG_{01} and SLG_{11} modes are plotted at different propagation distances in turbulent atmosphere, which are shown in Figs. 3 and 4 where $w_0 = 2$ cm, $\alpha_{0x} = \alpha_{0y} = 1$ cm, and $C_n^2 = 10^{-14}$ m$^{-2/3}$. A SLG_{11} mode in the source plane possesses the four-lobe structure. Each lobe spreads upon propagation in turbulent atmosphere. As a result, the space among the lobes diminishes and the lobes superpose upon the propagation. When the propagation distance z is an appropriate value, the SLG_{11} mode in turbulent atmosphere

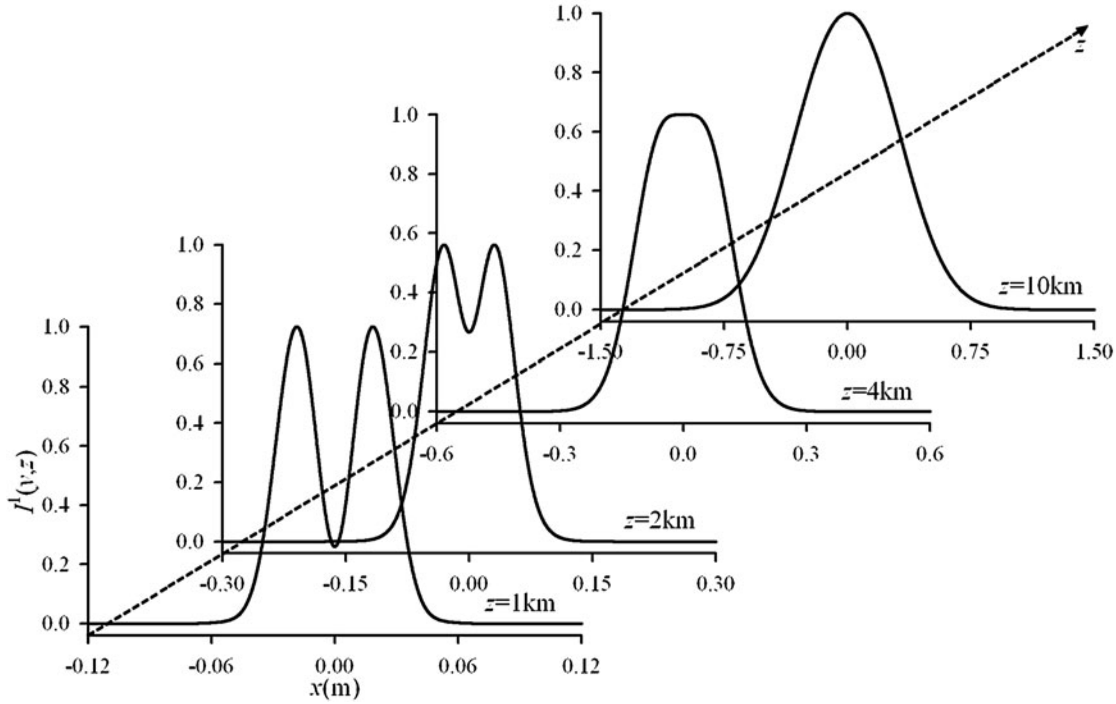

Fig. 2 Normalized average intensity distributions in the y-direction of a SLG_{01} mode at different propagation distances in turbulent atmosphere. $w_0 = 2$ cm, $\alpha_{0y} = 1$ cm, and $C_n^2 = 10^{-14}$ m$^{-2/3}$

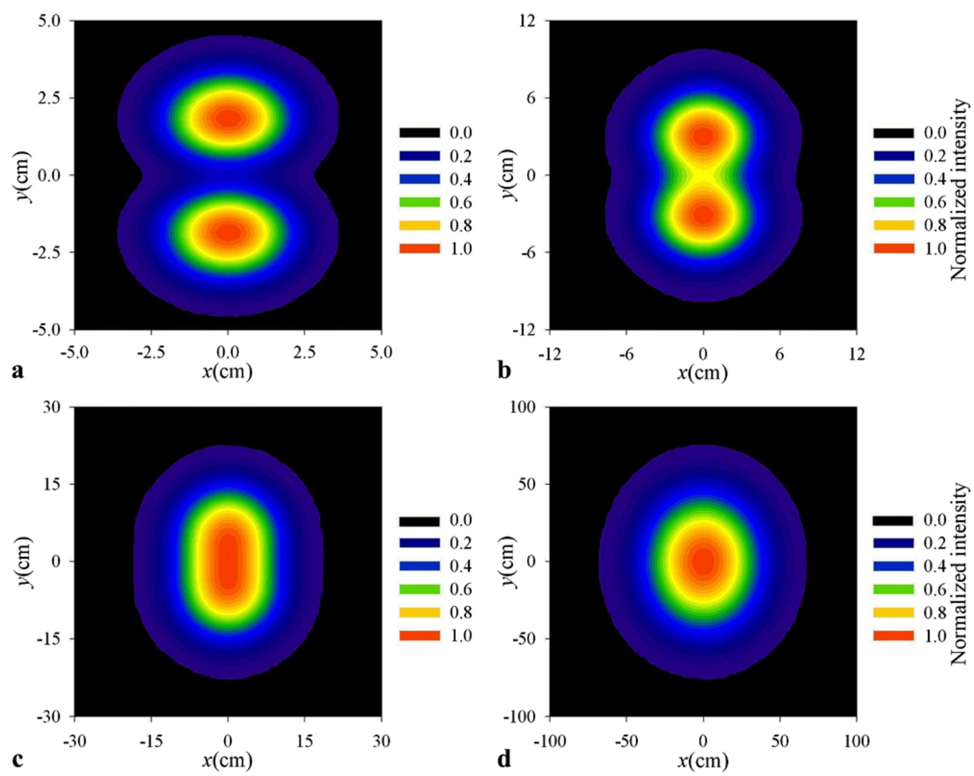

Fig. 3 Contour graphs of normalized intensity distribution of a SLG_{01} mode at different propagation distances in turbulent atmosphere. $w_0 = 2$ cm, $\alpha_{0x} = \alpha_{0y} = 1$ cm, and $C_n^2 = 10^{-14}$ m$^{-2/3}$. (**a**) $z = 1$ km. (**b**) $z = 2$ km. (**c**) $z = 4$ km. (**d**) $z = 10$ km

becomes a flattened beam spot. The process of evolvement of SLG_{01} and SLG_{11} modes in turbulent atmosphere is given in Figs. 3 and 4.

To further reveal the spreading property of a SLG_{01} mode in turbulent atmosphere, the effective beam sizes in the x- and y-directions of a SLG_{01} mode versus the prop-

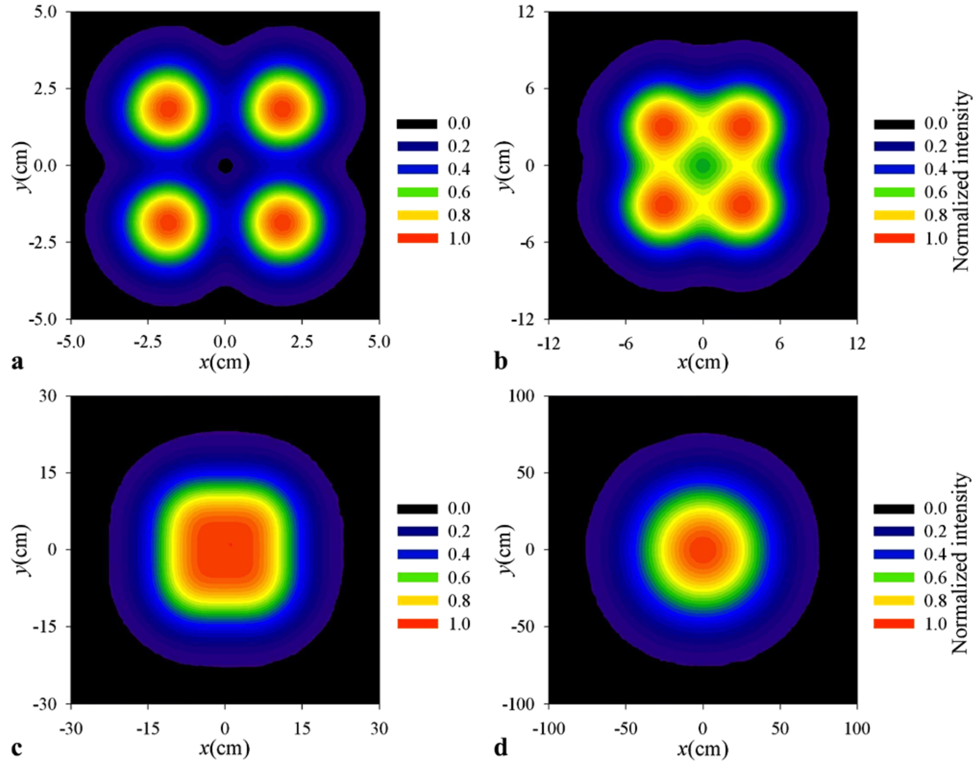

Fig. 4 Contour graphs of normalized intensity distribution of a SLG_{11} mode at different propagation distances in turbulent atmosphere. $w_0 = 2$ cm, $\alpha_{0x} = \alpha_{0y} = 1$ cm, and $C_n^2 = 10^{-14}$ $m^{-2/3}$. (**a**) $z = 1$ km. (**b**) $z = 2$ km. (**c**) $z = 4$ km. (**d**) $z = 10$ km

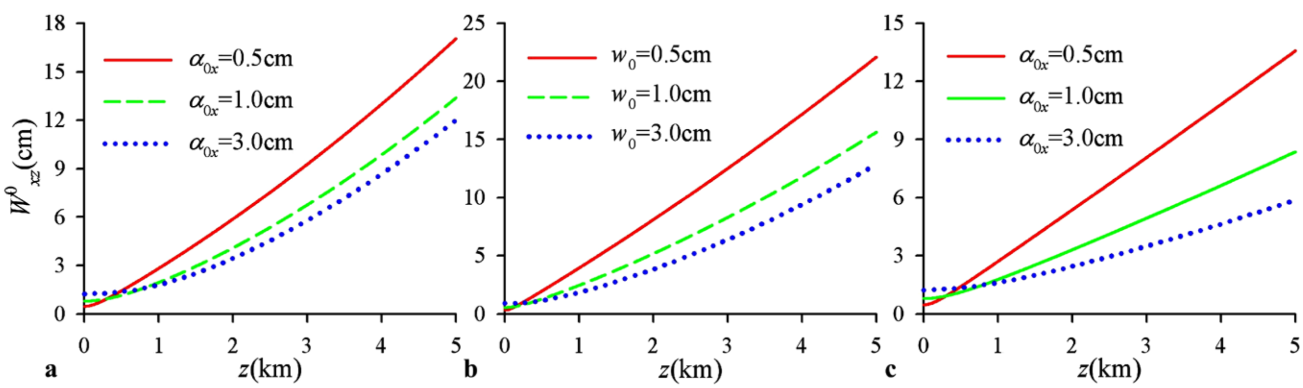

Fig. 5 The effective beam size in the x-direction of a SLG_{01} mode versus the propagation distance z in turbulent atmosphere. (**a**) $w_0 = 2$ cm and $C_n^2 = 10^{-14}$ $m^{-2/3}$. (**b**) $\alpha_{0x} = 1$ cm and $C_n^2 = 10^{-14}$ $m^{-2/3}$. (**c**) $w_0 = 2$ cm and $C_n^2 = 10^{-15}$ $m^{-2/3}$

agation distance z in turbulent atmosphere are depicted in Figs. 5 and 6. In Figs. 5(a) and 6(a), $w_0 = 2$ cm and $C_n^2 = 10^{-14}$ $m^{-2/3}$. $\alpha_{0x} = 1$ cm and $C_n^2 = 10^{-14}$ $m^{-2/3}$ in Figs. 5(b) and 6(b). In Fig. 5(c), $w_0 = 2$ cm and $C_n^2 = 10^{-15}$ $m^{-2/3}$. $w_0 = 2$ cm and $C_n^2 = 10^{-13}$ $m^{-2/3}$ in Fig. 6(c). With the same w_0, a SLG_{01} mode with the smaller α_{0x} spreads more rapidly in the x-direction. With the same α_{0x}, a SLG_{01} mode with the smaller w_0 spreads more quickly in the x-direction. Comparing Fig. 5(a) with Fig. 5(c), we can find that a SLG_{01} mode in turbulent atmosphere for a larger structure constant spreads more rapidly in the x-direction. With the same w_0, however, a SLG_{01} mode with the larger α_{0y} spreads more rapidly in the y-direction. With the same α_{0y}, a SLG_{01} mode with the larger w_0 spreads more quickly in the y-direction. This difference can be interpreted as follow. A SLG_{01} mode in the source plane possesses the two-lobe structure. The larger w_0 or α_{0y} is, the larger the space between the two lobes in the source plane is. Upon propagation in turbulent atmosphere, the space between the two lobes decreases as the two lobes spread. When $z = 2$ km, the two lobes superpose. Therefore, a SLG_{01} mode with the larger w_0 or α_{0y} has a larger beam spot in the y-direction, which is caused by the isotropic influence of the atmosphere turbulence and the zero central intensity in the source plane. Figures 6(a) and 6(c) denote that a SLG_{01} mode in turbulent atmosphere for a larger

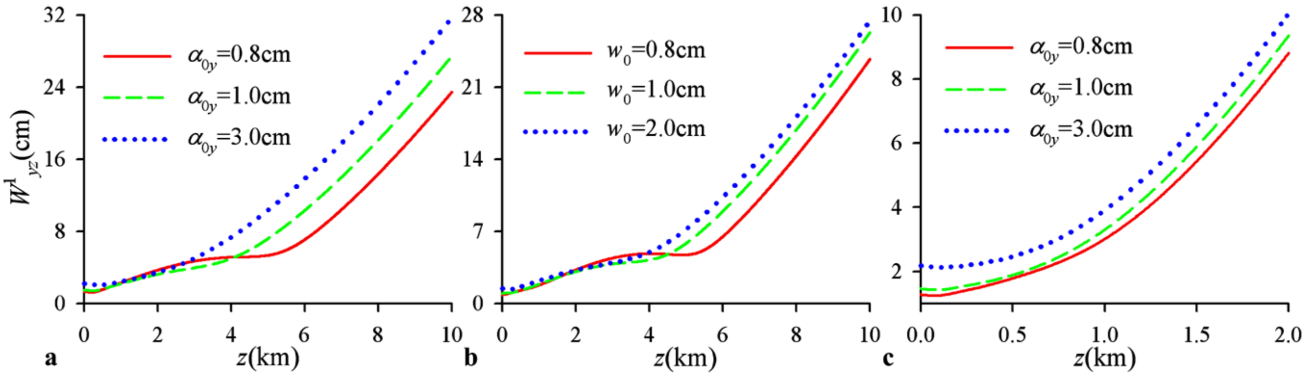

Fig. 6 The effective beam size in the y-direction of a SLG_{01} mode versus the propagation distance z in turbulent atmosphere. (**a**) $w_0 = 2$ cm and $C_n^2 = 10^{-14}$ m$^{-2/3}$. (**b**) $\alpha_{0y} = 1$ cm and $C_n^2 = 10^{-14}$ m$^{-2/3}$. (**c**) $w_0 = 2$ cm and $C_n^2 = 10^{-13}$ m$^{-2/3}$

structure constant spreads more rapidly in the y-direction. The spreading property of a SLG_{11} mode in turbulent atmosphere is the same as that in the y-direction of a SLG_{01} mode, and the corresponding figures are omitted here.

4 Conclusions

Based on the extended Huygens–Fresnel integral and the expansion of Lorentzian distribution, analytical expressions of the average intensities of SLG_{01} and SLG_{11} modes are derived in turbulent atmosphere, respectively. Also, the analytical formulae of the effective beam sizes of SLG_{01} and SLG_{11} modes in turbulent atmosphere are presented. The dependence of the propagation of SLG_{01} and SLG_{11} modes in turbulent atmosphere on the beam parameters and the structure constant of the atmospheric turbulence are analyzed. The analytical formulae of the average intensity and the effective beam size derived above seem to be very complicated. However, the weight coefficients in (8) and (9) decay rapidly, therefore the calculations of the average intensity and the effective beam size are fast. As to other complicated SLG modes, their propagation properties in turbulent atmosphere can be analyzed by the same procedure as here. This research is useful to the optical communications involving the multi-mode diode lasers.

Acknowledgements This research was supported by National Natural Science Foundation of China under Grant No. 10974179 and Zhejiang Provincial Natural Science Foundation of China under Grant No. Y1090073.

References

1. A. Naqwi, F. Durst, Appl. Opt. **29**, 1780 (1990)
2. J. Yang, T. Chen, G. Ding, X. Yuan, Proc. SPIE **6824**, 68240A (2008)
3. O.E. Gawhary, S. Severini, J. Opt. A, Pure Appl. Opt. **8**, 409 (2006)
4. O.E. Gawhary, S. Severini, Opt. Commun. **269**, 274 (2007)
5. A. Torre, W.A.B. Evans, O.E. Gawhary, S. Severini, J. Opt. A, Pure Appl. Opt. **10**, 115007 (2008)
6. G. Zhou, Appl. Phys. B **93**, 891 (2008)
7. G. Zhou, J. Opt. Soc. Am. A **25**, 2594 (2008)
8. G. Zhou, J. Opt. Soc. Am. B **26**, 141 (2009)
9. G. Zhou, J. Opt. Soc. Am. A **26**, 350 (2009)
10. G. Zhou, Appl. Phys. B **96**, 149 (2009)
11. P. Zhou, X. Wang, Y. Ma, H. Ma, X. Xu, Z. Liu, J. Opt. **12**, 015409 (2010)
12. G. Zhou, J. Opt. Soc. Am. A **27**, 563 (2010)
13. H.T. Eyyuboğlu, Y. Baykal, Appl. Opt. **44**, 976 (2005)
14. H.T. Eyyuboğlu, J. Opt. Soc. Am. A **22**, 1527 (2005)
15. Y. Cai, S. He, Opt. Express **14**, 1353 (2006)
16. Y. Cai, Y. Chen, H.T. Eyyuboğlu, Y. Baykal, Opt. Lett. **32**, 2405 (2007)
17. G. Zhou, Opt. Express **16**, 3504 (2008)
18. Y. Cai, O. Korotkova, H.T. Eyyuboğlu, Y. Baykal, Opt. Express **16**, 15834 (2008)
19. Y. Zhu, D. Zhao, X. Du, Opt. Express **16**, 18437 (2008)
20. Y. Zhu, D. Zhao, J. Opt. Soc. Am. A **25**, 773 (2008)
21. Y. Yuan, Y. Cai, J. Qu, H.T. Eyyuboğlu, Y. Baykal, Opt. Express **17**, 11130 (2009)
22. D. Zhao, X. Du, Opt. Express **17**, 4257 (2009)
23. P.P. Schmidt, J. Phys. B, At. Mol. Phys. **9**, 2331 (1976)
24. I.S. Gradshteyn, I.M. Ryzhik, *Table of Integrals, Series, and Products* (Academic Press, New York, 1980)